SUPPORTING INFORMATION

A Comparison of Experimental and Broken Symmetry Density Functional Theory (BS-DFT) Calculated Electron Paramagnetic Resonance (EPR) Parameters for the Manganese Catalase Active Site in the Superoxidised Mn^{III}/Mn^{IV} State

Nathan J Beal, Thomas Corry and Patrick J O'Malley*

School of Chemistry, The University of Manchester, Manchester M13 9PL, UK.

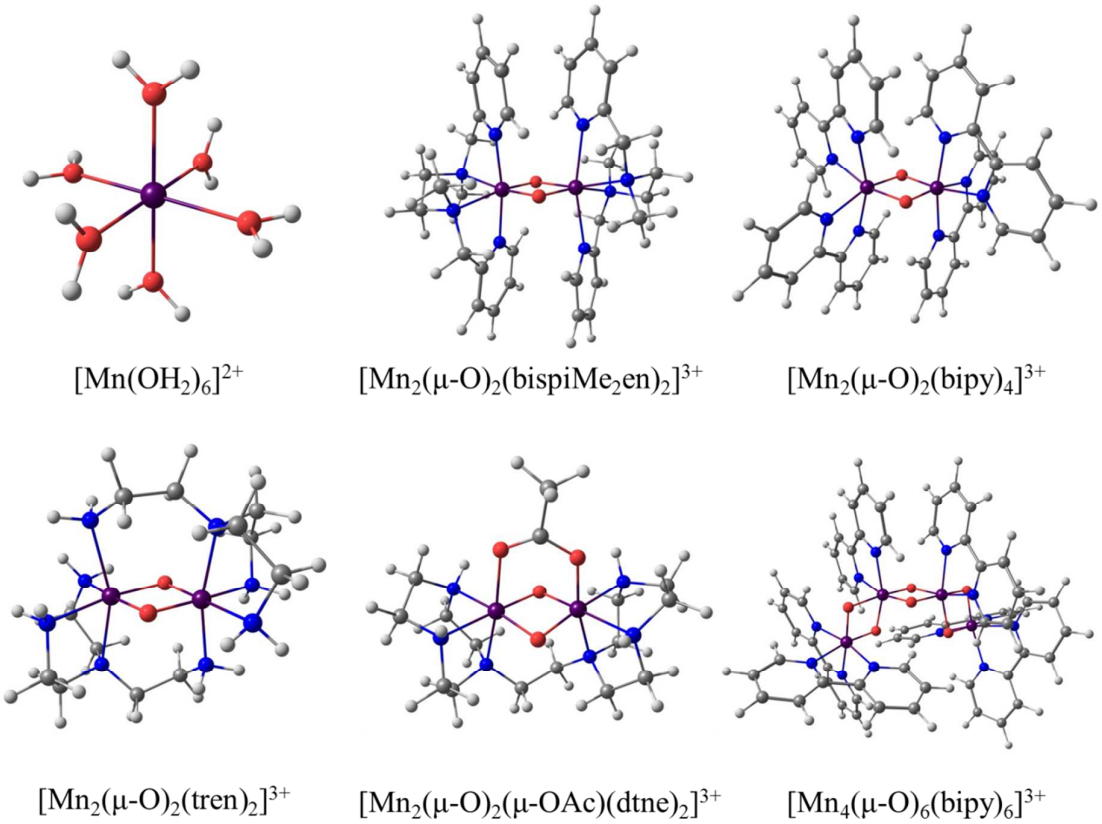

Figure S1 Optimised structures of the mononuclear, dinuclear and tetranuclear manganese model complexes used for the empirically determined scaling factor applied to the isotropic metal hyperfine coupling (see section 5.2). Where bispiMe2en = N,N′-dimethyl-N,N′-bis(2-pyridyl- methyl)ethane-1,2-diamine, bipy = 2,2'-bipyridine and tren = tris(2-aminoethyl)amine. Colour coding: manganese (purple), oxygen (red), nitrogen (blue), carbon (grey) and hydrogen (white).

Table S1. Calculated and experimental ^{55}Mn isotropic hyperfine couplings (in MHz) for the model complexes displayed in Figure S2, used to calculate the empirical scaling factor f_{iso} to be applied to BS-DFT calculated ^{55}Mn isotropic hyperfine couplings.

Complex	Oxidation State	A_{iso}(calc.)	A_{iso}(exp.)	f_{iso}	Ref.
$[Mn(OH_2)_6]^{2+}$	Mn^{II}	−192	−264	1.38	[1]
$[Mn_2(\mu\text{-}O)_2(bispiMe_2en)_2]^{3+}$	Mn^{III}	−291	−408	1.40	[2]
	Mn^{IV}	141	−230	1.63	[2]
$[Mn_2(\mu\text{-}O)_2(bipy)_4]^{3+}$	Mn^{III}	−306	−452	1.47	[3]
	Mn^{IV}	141	−219	1.56	[3]
$[Mn_2(\mu\text{-}O)_2(tren)_2]^{3+}$	Mn^{III}	−268	−428	1.60	[4]
	Mn^{IV}	138	−207	1.50	[4]
$[Mn_2(\mu\text{-}O)_2(\mu\text{-}OAc)(dtne)_2]^{3+}$	Mn^{III}	−248	−391	1.57	[3]
	Mn^{IV}	141	−209	1.49	[3]
$[Mn_4(\mu\text{-}O)_6(bipy)_6]^{3+}$	Mn^{III}	−255	−449	1.76	[5]
	Mn^{IV}	171	228	1.34	[5]
	Mn^{IV}	−179	−189	1.05	[5]
	Mn^{IV}	123	172	1.40	[5]
			Average f_{iso}	1.47	

Table S2. Calculated and experimental ^{17}O hyperfine couplings (in MHz) for the bridging oxygens for the multinuclear complexes featured in Figure S2. Calculated ^{17}O hyperfine couplings are computed using the averaged spin projection methodology.[6,7]

	Label	A_{iso}	T_1	T_2	T_3
$[Mn_2(\mu\text{-}O)_2(bispiMe_2en)_2]^{3+}$	O_1	3.4	−22.7	8.6	14.1
	O_2	3.3	−22.7	8.6	14.0
$[Mn_2(\mu\text{-}O)_2(bipy)_4]^{3+}$	O_1	3.5	−23.6	8.2	15.4
	O_2	3.5	−23.6	8.2	15.4
$[Mn_2(\mu\text{-}O)_2(tren)_2]^{3+}$	O_1	4.1	−21.5	10.1	11.4
	O_2	3.9	−21.6	10.4	11.2
$[Mn_2(\mu\text{-}O)_2(\mu\text{-}OAc)(dtne)_2]^{3+}$	O_1	2.7	−20.9	7.6	13.3
	O_2	2.4	−21.3	7.8	13.5
$[Mn_4(\mu\text{-}O)_6(bipy)_6]^{3+}$	O_1	−1.8	−14.8	−1.8	16.7
	O_2	−2.9	−15.6	−0.1	15.7
	O_3	−3.6	−11.6	−3.1	14.7
	O_4	−2.0	−10.5	−6.1	16.6
	O_5	6.5	−21.0	3.9	17.1
	O_6	6.7	−17.8	2.7	15.1
	Exp.[8]				
$[Mn_2(\mu\text{-}O)_2(bipy)_4]^{3+}$	bridge	5.1	−18.5	6.4	12.0
$[Mn_2(\mu\text{-}O)_2(\mu\text{-}OAc)(dtne)_2]^{3+}$	bridge	5.3	−18.8	6.2	11.6

Table S3. Calculated and experimental ^{17}O hyperfine couplings (in MHz) for the bridging oxygens for the multinuclear complexes featured in Figure S2. Calculated ^{17}O hyperfine couplings are computed using the summed spin projection methodology.[8]

	Label	A_{iso}	T_1	T_2	T_3
$[Mn_2(\mu\text{-}O)_2(bispiMe_2en)_2]^{3+}$	O_1	6.8	−45.3	17.2	28.1
	O_2	6.6	−45.3	17.2	28.1
$[Mn_2(\mu\text{-}O)_2(bipy)_4]^{3+}$	O_1	7.0	−47.2	16.4	30.8
	O_2	7.0	−47.2	16.4	30.8
$[Mn_2(\mu\text{-}O)_2(tren)_2]^{3+}$	O_1	8.2	−42.9	20.2	22.8
	O_2	7.7	−43.3	20.9	22.4
$[Mn_2(\mu\text{-}O)_2(\mu\text{-}OAc)(dtne)_2]^{3+}$	O_1	5.3	−41.9	15.2	26.7
	O_2	4.8	−42.6	15.6	26.9
$[Mn_4(\mu\text{-}O)_6(bipy)_6]^{3+}$	O_1	−3.5	−29.6	−3.7	33.3
	O_2	−5.7	−31.2	−0.1	31.3
	O_3	−7.2	−23.2	−6.2	29.4
	O_4	−4.0	−21.0	−12.2	33.2
	O_5	13.0	−19.4	3.6	15.8
	O_6	13.5	−16.4	2.4	13.9
	Exp.[8]				
$[Mn_2(\mu\text{-}O)_2(bipy)_4]^{3+}$	bridge	5.1	−18.5	6.4	12.0
$[Mn_2(\mu\text{-}O)_2(\mu\text{-}OAc)(dtne)_2]^{3+}$	bridge	5.3	−18.8	6.2	11.6

References

(1) Luckhurst, G. R.; Pedulli, G. F. Electron Spin Relaxation in Solutions of Manganese (II) Ions. *Mol. Phys.* **1971**, *22* (5), 931–935.

(2) Hureau, C.; Blondin, G.; Cesario, M.; Un, S. Direct Measurement of the Hyperfine

and G -Tensors of a Mn(III)−Mn(IV) Complex in Polycrystalline and Frozen Solution Samples by High-Field EPR. *J. Am. Chem. Soc.* **2003**, *125* (38), 11637–11645.

(3) Schäfer, K.-O.; Bittl, R.; Zweygart, W.; Lendzian, F.; Haselhorst, G.; Weyhermüller, T.; Wieghardt, K.; Lubitz, W. Electronic Structure of Antiferromagnetically Coupled Dinuclear Manganese (Mn III Mn IV) Complexes Studied by Magnetic Resonance Techniques. *J. Am. Chem. Soc.* **1998**, *120* (50), 13104–13120.

(4) Horner, O.; Charlot, M.-F.; Boussac, A.; Anxolabéhère-Mallart, E.; Tchertanov, L.; Guilhem, J.; Girerd, J.-J. Synthesis, Structure, Electronic, Redox, and Magnetic Properties of a New Mixed-Valent Mn-Oxo Cluster: [Mn2III,IVO2(N,Nbispicen)2]3+ (N,Nbispicen =N,N-bis(2-Pyridylmethyl)-1,2-Diaminoethane). *Eur. J. Inorg. Chem.* **1998**, *1998* (6), 721–727.

(5) Blondin, G.; Davydov, R.; Philouze, C.; Charlot, M.; Styring, S.; Åkermark, B.; Girerd, J.; Boussac, A. Electron Paramagnetic Resonance Study of the S = ½ Ground State of a Radiolysis-Generated manganese(III)–trimanganese(IV) Form of [MnIV4O6(bipy)6]4+ (Bipy = 2,2′-Bipyridine). Comparison with the Photosynthetic Oxygen Evolving Complex †. *J. Chem. Soc. Dalt. Trans.* **1997**, *6* (21), 4069–4074.

(6) Han, W.-G. W.; Liu, T.; Lovell, T.; Noodleman, L. Active Site Structure of Class I Ribonucleotide Reductase Intermediate X: A Density Functional Theory Analysis of Structure, Energetics, and Spectroscopy. *J. Am. Chem. Soc.* **2005**, *127* (45), 15778–15790.

(7) Han, W.-G.; Noodleman, L. DFT Calculations of Comparative Energetics and ENDOR/Mössbauer Properties for Two Protonation States of the Iron Dimer Cluster of Ribonucleotide Reductase Intermediate X. *Dalt. Trans.* **2009**, No. 30, 6045.

(8) Rapatskiy, L.; Ames, W.; Pérez-Navarro, M.; Savitsky, A.; Griese, J. J.; Weyhermüller, T.; Shafaat, H. S.; Högbom, M.; Neese, F.; Pantazis, D. A.; et al. Characterization of Oxygen Bridged Manganese Model Complexes Using Multifrequency ^{17}O-Hyperfine EPR Spectroscopies and Density Functional Theory. *J. Phys. Chem. B* **2015**, *119* (43), 13904–13921.